2014 3rd International Conference on Environment, Chemistry and Biology
IPCBEE vol.78 (2014) © (2014) IACSIT Press, Singapore
DOI: 10.7763/IPCBEE. 2014. V78. 17

Assessment of Wall Shear Stress and Arteriolar Network Architecture in Rat Skeletal Muscle Using Biomicroscopy

Elena Kostromina [1+]

[1] Moscow State University, Moscow, Russian Federation

Abstract. Understanding the mechanisms underlying the regulation of vessel diameter and blood flow in the microcirculation is critically important for studying adaptive responses in microvascular networks, and therefore, could facilitate the development of treatment strategies for vascular disorders. Wall shear stress (WSS) induced by blood flow is considered a significant factor determining the architecture of the microvascular bed; however, the mechanisms regulating this process are not completely understood. The aim of this study was to estimate WSS values in arterioles of different sizes and locations within a microvascular bed, and to establish the relationship between WSS, wall-to-lumen ratio (WLR), and other microcirculatory parameters in the rat skeletal muscle microvasculature under normal physiological conditions. To perform quantitative analysis, data obtained from intravital microscopic examination of 14 microvascular networks were used. Wall thickness, WLR, WSS, and blood flow were estimated in arteriolar segments, for which the outer and inner diameters, blood flow velocity, and location within the network were determined. It was found that along the arteriolar tree, WSS varied within a wide range, and a direct correlation between WLR and WSS was revealed. The established relationship between WLR and WSS points to the coupled roles of transmural pressure and shear stress in the development and adaptation of arteriolar networks, and could be used for the development of computational models of terminal vascular beds.

Keywords: arteriole, blood flow, microvascular networks, shear stress, wall-to-lumen ratio

1. Introduction

Arteriolar networks are designed for the delivery of blood to certain tissue areas and the adjustment of local blood flow to support the metabolic needs of surrounding tissues [1], [2]. Regulation of blood flow in the microcirculatory system, employing changes in vascular resistance to blood flow, is the result of a coordinated adjustment of arteriolar diameters and is achieved by active responses of vascular wall elements to a large variety of different stimuli, including hemodynamic and metabolic factors [3]. The adjustment of luminal diameter employs changes in both vascular tone and the structures of resistance vessels, occurring within seconds to weeks [4]. Thus, in established hypertension, the increase in blood pressure correlates with a proportional increase in peripheral resistance: small arteries and arterioles are characterized by reduced inner diameters and increased wall-to-lumen ratio (WLR) both in hypertensive patients and in animal models of hypertension [5], [6]. Under normal physiological conditions, the heterogeneity of terminal arterioles in terms of WLR was previously reported to be essential for blood flow regulation, and WLR is known to be quantitatively related to vascular tone as well as the mechanical properties of arterioles and their reactivity in vasomotor reactions [7], [8]. At the same time, wall shear stress (WSS) induced by blood flow is considered an important factor affecting the architecture of vascular beds. According to the "pressure-shear" hypothesis, the design of vascular networks as well as the adaptive reactions of blood vessels result from the balance between shear stress and pressure [9]. However, the mechanisms of vascular diameter regulation are not completely understood. This study was undertaken to estimate the distribution of WSS values at different

[+]Corresponding author: Tel.: +7-495-7229247; fax: +7-495-7229247
E-mail address: rumed07@hotmail.com

levels of the rat skeletal muscle microvasculature and to establish relationships between shear stress, WLR, and other microcirculatory parameters under normal physiological conditions using biomicroscopy.

2. Materials and Methods

2.1. Experimental network data

Microvascular networks in the rat cremaster muscle have been studied using intravital microscopy. All animal experiments were conducted in accordance with the Guide for the Care and Use of Laboratory Animals (NIH, 1985) and national regulations. In this study, male Wistar rats with body weights between 75 and 110 g were used. All experimental procedures, including anaesthesia, animal preparation for biomicroscopy, blood pressure monitoring, and experimental setup, were previously described in detail [7].

Biomicroscopy was performed using an upright research microscope Orthoplan (Leitz, Germany) equipped with a long working distance condenser. General observations were conducted using ×2.5/0.08 and ×6.3/0.20 objectives; and examinations of single microvessels and measurements were carried out with SW ×50/1.0 and SW ×100/1.2 objectives. At the beginning of each experiment, images of a microvascular bed were taken to select areas for further microscopic assessment. Measurements of microvascular dimensions were performed using a digital linear micrometer RZD-DO (Leitz) with a transducer located in the 12.5× ocular. Blood flow velocity in the entire cross-section of arterioles was recorded by an MPV-Compact-Vel instrument (Leitz) using microprism grating method as described elsewhere [10], [11].

Wall thickness (W) and WLR were calculated as follows: W = (OD − ID)/2; WLR = (OD − ID)/ID, where OD and ID represent the outer and inner arteriole diameters, respectively. Blood flow rate (Q) in single microvessels was calculated from the measured mean blood flow velocity (V) and ID according to the formula: $Q = V * \pi * (ID/2)^2$. WSS was calculated according to Poiseuille's law from the equation $WSS = 32 * \eta * Q/(\pi * ID^3) = \eta * 8 * V/ID$ (1), where the viscosity of blood (η) was first considered constant and taken as 3.5×10^{-3} Pa ∗ s [12] (WSS^1) or calculated according to the "in vivo viscosity law" [13] as the product of the relative apparent viscosity (η_{vivo}) and the viscosity of rat plasma (η_{plasma}) (WSS^2) assuming that the hematocrit is equal to 45% (H_D = 0.45) and η_{plasma} is equal to 1.05×10^{-3} Pa ∗ s [14].

Therefore,

$$\eta = \eta_{plasma} * \eta_{vivo} = \eta_{plasma} * \{1 + (\eta^*_{0.45} - 1) * 1 * [ID/(ID - 1.1)]^2\} * [ID/(ID - 1.1)]^2 \quad (2)$$

where $\eta^*_{0.45}$ is calculated as follows:

$$\eta^*_{0.45} = 6 * e^{-0.085\,ID} + 3.2 - 2.44 * e^{-0.06\,ID^{0.645}} \quad (3)$$

2.2. Statistical analysis

Data are presented as mean ±SEM. The means were compared by one-way analysis of variance (ANOVA) using MegaStat software (USA). Post-hoc analysis of the P values from the pairwise t test allowed comparisons between each combination of two groups. The level of statistical significance was set at $P < 0.05$. Least squares linear regression was used to evaluate the correlation between parameters.

3. Results

3.1. Arteriolar network characterisation

Quantitative analysis of arteriolar networks in the rat cremaster muscle was done using measurement data obtained from microscopic examinations of 14 microvascular beds. All arterioles were classified into five orders of branching in accordance with their position within the vascular tree [15] and divided into groups according to their branching order. A representative fragment of the cremaster microcirculatory bed is shown in Figure 1. The arteriole designated in the first order of branching (1A) gives rise to several 2A arterioles, a number of 3A arterioles originate from one 2A arteriole, and so on. The results of the determination of hemodynamic parameters for 143 examined 1A–5A arterioles are presented in Table 1.

Arteriolar networks in the rat cremaster muscle represent a heterogeneous population of microvessels with lumen diameters varying more than 10-fold in size. Mean values of ID and V, which were recorded simultaneously, progressively declined with branching. W and WLR were determined for 103 examined arterioles (1A–4A), which contained continuous layers of smooth muscle cells, and the outer and inner borders of the arteriole walls were clearly distinguishable. Similar to lumen diameter, W gradually decreased

with branching; however, the mean value of ID decreased to a greater extent when compared to the average W decrease (6-fold versus 2.1-fold, respectively). Consistent with the results of the W and ID measurements, the average WLR was minimal in 1A arterioles and consequently increased with branching, reaching its maximum mean value in the 4A group.

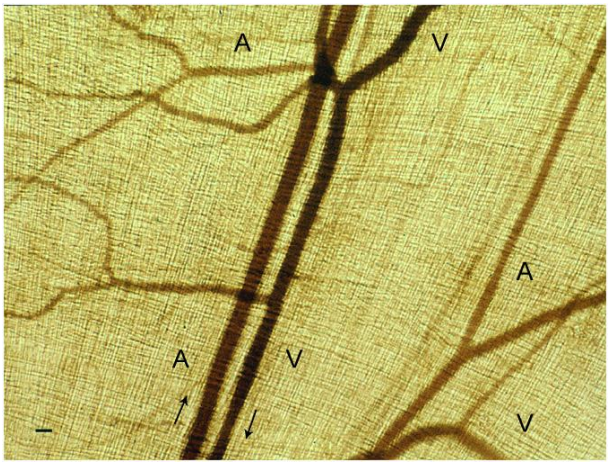

Fig. 1: A fragment of the microvascular bed of the rat cremaster muscle is shown. The first-order arteriole gives rise to several arterioles of the second order, and so on. A – arterioles; V – venules. Scale bar – 100 μm. Objective 6.3×/0.20. The direction of blood flow is indicated by the arrows.

Table 1: Microcirculatory parameters in arterioles of different branching orders

Parameter	1A arterioles	2A arterioles	3A arterioles	4A arterioles	5A arterioles
ID, μm	100.7 ± 3.1 (14)	70.9 ± 1.8 (41)^{a1}	34.8 ± 1.9 (44)^{b1}	16.9 ± 1.4 (29)^{c1}	9.7 ± 0.7 (15)^{d2}
V, mm/s	7.1 ± 0.2 (14)	6.3 ± 0.1 (41) $^{\#}$	5.8 ± 0.2 (44)^{a2}	4.9 ± 0.3 (29)^{c2}	3.2 ± 0.4 (15)^{d1}
W, μm	13.5 ± 0.8 (7)	10.7 ± 0.5 (38)^{a2}	8.0 ± 0.3 (43)^{b1}	6.4 ± 0.4 (15)^{c2}	
WLR	0.27 ± 0.01 (7)	0.30 ± 0.01 (38)^{NS}	0.52 ± 0.04 (43)^{b1}	0.63 ± 0.04 (15)^{c2}	
WSS^1, N/m^2	2.0 ± 0.1 (7)	2.5 ± 0.1 (38)^{NS}	5.3 ± 0.5 (43)^{b1}	7.5 ± 0.6 (15)^{c2}	
WSS^2, N/m^2	1.5 ± 0.1 (7)	1.8 ± 0.1 (38)^{NS}	4.7 ± 0.6 (43)^{b1}	7.7 ± 0.9 (15)^{c2}	

Data are presented as means ± SEM, (number of measurements); $^{a1, a2}$ P<0.001, P<0.05 compared to 1A; $^{b1, b2}$ P<0.001, P<0.05 compared to 2A; $^{c1, c2}$ P<0.001, P<0.05 compared to 3A; $^{d1, d2}$ P<0.001, P<0.05 compared to 4A, respectively. ^{NS} the difference was not statistically significant; $^{\#}$ P = 0.055.

3.2. Determination of WSS in arterioles

Shear stresses in arteriolar segments were estimated from equation 1, using two different approaches. First, we assumed that blood viscosity is constant and calculated WSS using an effective value of blood viscosity equal to 3.5×10^{-3} Pa * s [12] and the measured luminal diameter and V in arterioles. The lowest calculated mean WSS value was determined in 1A arterioles (2.0 ± 0.1 N/m^2), gradually increased with vessel branching, and reached its maximum value (7.5 ± 0.6 N/m^2) in 4A arterioles. Second, as the apparent viscosity of blood flowing through the microvasculature depends on a number of physiological factors, including hematocrit and vessel diameter, blood viscosity was calculated according to the "in vivo viscosity law" [13] from a parametric equation proposed for the variation of viscosity with luminal diameter and assuming hematocrit equal to 45%. Similar to the previous approach, mean shear stresses, calculated using "in vivo viscosity" estimates, gradually increased with branching and reached its maximum (7.7 ± 0.9 N/m^2) in 4A arterioles. Along the arteriolar tree, WSS varied more than 10-fold.

To investigate the relationship between WLR and shear stress, WLR was considered as a function of WSS, which was calculated first for blood viscosity taken as 3.5×10^{-3} Pa * s (Fig. 2A) and then for blood viscosity determined according to the "in vivo viscosity law" (Fig. 2B) for 103 1A–4A arterioles. In both cases, WLR gradually increased as WSS increased, and a significant linear relationship was established between WLR and WSS ($R^2 = 0.644$, $p<0.001$ and $R^2 = 0.687$, $p<0.001$, respectively; Fig. 2A and Fig. 2B). Thus, the analysis revealed a correlation between WLR and WSS, which allows us to use the equations for the development of computational models of arteriolar networks.

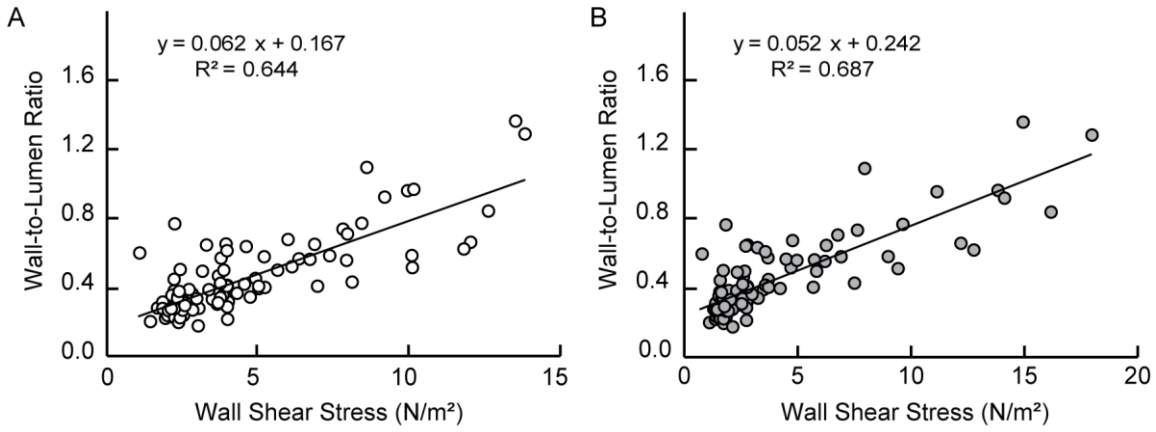

Fig. 2: Relationship between wall-to-lumen ratio and wall shear stress (WSS) for arterioles of different branching orders. A. WSS was calculated assuming that blood viscosity was constant and equal to 3.5×10^{-3} Pa*s. B. WSS was determined for blood viscosity calculated according to the "in vivo viscosity law" (equation 2). Lines represent the linear regression best fit for A ($p<0.001$; $n = 103$) and B ($p<0.001$; $n = 103$). Linear regression equations and R^2 are presented.

4. Discussion

Investigation of mechanisms underlying the regulation of vascular diameter under normal conditions is critically important for the understanding of adaptive responses in the microcirculation and could facilitate the development of treatment strategies for vascular disorders. Using data obtained from microscopic examinations of the rat skeletal muscle microvasculature, the distributions of the microcirculatory parameters within arteriolar networks were determined, and a direct correlation between WLR and WSS was revealed. Since the parameters were recorded in a tissue with normal vascular tone, the observed relationship between WLR and shear stress reflect both structural and functional arteriole properties [7] that result from long-term adaptations of the microvascular network.

Microvascular network formation is controlled by multiple molecular signals [16]; numerous knockout animal studies have revealed important roles for a large number of genes regulating blood vessel formation and vascular network function in different organs and tissues [17]-[20]. At the same time, vascular systems must adapt continuously to changing functional needs of organs and tissues to maintain their angioarchitecture and create appropriate hemodynamic conditions. Shear stress is considered to play a significant role in microvascular adaptation [21]. However, the experiments performed earlier by Bakker and others [22] showed that cremaster arterioles do not match their diameters solely to the level of shear stress. According to the "pressure-shear" hypothesis, the design of the vascular beds is the result of the balance between the effects of pressure and flow on the adaptive response of single vessels [9]. Taking into consideration that diameter changes are determined by active responses of vascular wall elements exposed to mechanical forces generated by shear stress and pressure [23], we estimated the values of WSS and WLR, which is a parameter directly proportional to the transmural pressure and inversely proportional to the circumferential wall stress according to the law of Laplace. A direct correlation revealed between WLR and WSS in arterioles of different branching orders supports the notion of coupled roles for blood pressure and WSS in the development, adaptation, and function of microvascular networks. However, future studies are

needed to address these complex questions. The established relationships between WLR and WSS could be used for the development of computational models of terminal vascular beds.

5. References

[1] T.W. Secomb, *Theoretical models for regulation of blood flow.* Microcirculation, 2008. **15**(8): p. 765-75

[2] R. N. Pittman, in *Regulation of Tissue Oxygenation*. 2011: San Rafael (CA).

[3] P. Johnson, *Overview of the microcirculation*, in *Handbook of Physiology: Microcirculation*, D.W.L.K. Tuma RF, Editor. 2008, Academic Press: San Diego, CA, USA. p. xi–xxiv.

[4] A. S. Popel, and P. C. Johnson, *Microcirculation and Hemorheology.* Annu Rev Fluid Mech, 2005. **37**: p. 43-69.

[5] P. I. Korner, *Essential hypertension and its causes: Neural and non-neural mechanisms*. 2007: Oxford University Press New York.

[6] M. J. Mulvany, *Small artery remodelling in hypertension: causes, consequences and therapeutic implications.* Med Biol Eng Comput, 2008. **46**(5): p. 461-7.

[7] E. Y. Kostromina, I.M. Rodionov, and V.S. Shinkarenko, *Tone, autoregulatory properties, and wall thickness-to-radius ratio in skeletal muscle arterioles.* Am J Physiol, 1991. **261**(4 Pt 2): p. H1095-101.

[8] I. M. Rodionov, O. S. Tarasova, and V.B. Koshelev, *Adaptation of resistance vessels to the transmural pressure level.* Ross Fiziol Zh Im I M Sechenova, 2001. **87**(11): p. 1477-87.

[9] A. R. Pries, T.W. Secomb, and P. Gaehtgens, *Design principles of vascular beds.* Circ Res, 1995. **77**(5): p. 1017-23.

[10] V. Shinkarenko, et al., *Studies of blood flow velocity in different parts of the mesenteric microvascular bed using MPV-Compact-Vel*, in *New Methods and Instruments for Microscopy in Biology and Medicine*, V. Shinkarenko, Editor. 1987: Wetzlar. p. 170-175.

[11] G. Mchedlishvili, et al., *Microcirculatory stasis induced by hemorheological disorders: further evidence.* Microcirculation, 1999. **6**(2): p. 97-106.

[12] H. H. Lipowsky, *Shear stress in the circulation*, in *Flow-Dependent Regulation of Vascular Function*. 1995, Springer. p. 28-45.

[13] A. R. Pries, et al., *Resistance to blood flow in microvessels in vivo.* Circ Res, 1994. **75**(5): p. 904-15.

[14] A. R. P ries, T. W. Secomb, and P. Gaehtgens, *Biophysical aspects of blood flow in the microvasculature.* Cardiovasc Res, 1996. **32**(4): p. 654-67.

[15] M. P. Wiedeman, *Blood flow through terminal arterial vessels after denervation of the bat wing*. Circ Res, 1968. **22**(1): p. 83-9.

[16] S. Lehoux, Y. Castier, and A. Tedgui, *Molecular mechanisms of the vascular responses to haemodynamic forces.* J Intern Med, 2006. **259**(4): p. 381-92.

[17] P. Carmeliet, and D. Collen, *Transgenic mouse models in angiogenesis and cardiovascular disease.* J Pathol, 2000. **190**(3): p. 387-405.

[18] E. Kostromina, X. Wang, and W. Han, *Altered islet morphology but normal islet secretory function in vitro in a mouse model with microvascular alterations in the pancreas.* PLoS One, 2013. **8**(7): p. e71277.

[19] E. Kostromina, et al., *Glucose intolerance and impaired insulin secretion in pancreas-specific signal transducer and activator of transcription-3 knockout mice are associated with microvascular alterations in the pancreas.* Endocrinology, 2010. **151**(5): p. 2050-9.

[20] T. Tanaka, and M. Nangaku, *Angiogenesis and hypoxia in the kidney.* Nat Rev Nephrol, 2013. **9**(4): p. 211-22.

[21] D. J. Green, et al., *Exercise and vascular adaptation in asymptomatic humans.* Experimental Physiology, 2011. **96**(2): p. 57-70.

[22] E. N. Bakker, et al., *Differential structural adaptation to haemodynamics along single rat cremaster arterioles.* J Physiol, 2003. **548**(Pt 2): p. 549-55.

[23] A. R. Pries, M. J. Mulvany, and E.N. Bakker, *MBEC special issue on microcirculation." engineering principles of vascular networks".* Med Biol Eng Comput, 2008. **46**(5): p. 407-9.